8112–8128 *Nucleic Acids Research, 2016, Vol. 44, No. 17* *Published online 25 May 2016*
doi: 10.1093/nar/gkw472

BAP18 coactivates androgen receptor action and promotes prostate cancer progression

Shiying Sun[1], Xinping Zhong[2], Chunyu Wang[1], Hongmiao Sun[1], Shengli Wang[1], Tingting Zhou[1], Renlong Zou[1], Lin Lin[1], Ning Sun[1], Ge Sun[1], Yi Wu[1], Botao Wang[3], Xiaoyu Song[1], Liu Cao[1] and Yue Zhao[1,*]

[1]Department of Cell Biology, Key laboratory of Cell Biology, Ministry of Public Health, and Key laboratory of Medical Cell Biology, Ministry of Education, China Medical University, Shenyang, Liaoning 110122, China, [2]Department of General Surgery, the First Affiliated Hospital, China Medical University, Shenyang, Liaoning 110001, China and [3]School of Computer Science and Engineering, Northeastern University, Shenyang, Liaoning 110004, China

Received October 13, 2015; Revised May 12, 2016; Accepted May 14, 2016

ABSTRACT

BPTF associated protein of 18 kDa (BAP18) has been reported as a component of MLL1-WDR5 complex. However, BAP18 is an uncharacterized protein. The detailed biological functions of BAP18 and underlying mechanisms have not been defined. Androgen receptor (AR), a member of transcription factor, plays an essential role in prostate cancer (PCa) and castration-resistant prostate cancer (CRPC) progression. Here, we demonstrate that BAP18 is identified as a coactivator of AR in *Drosophilar* experimental system and mammalian cells. BAP18 facilitates the recruitment of MLL1 subcomplex and AR to androgen-response element (ARE) of AR target genes, subsequently increasing histone H3K4 trimethylation and H4K16 acetylation. Knockdown of BAP18 attenuates cell growth and proliferation of PCa cells. Moreover, BAP18 depletion results in inhibition of xenograft tumor growth in mice even under androgen-depletion conditions. In addition, our data show that BAP18 expression in clinical PCa samples is higher than that in benign prostatic hyperplasia (BPH). Our data suggest that BAP18 as an epigenetic modifier regulates AR-induced transactivation and the function of BAP18 might be targeted in human PCa to promote tumor growth and progression to castration-resistance.

INTRODUCTION

Androgen receptor (AR) is an important ligand-dependent transcriptional factor, which is required for development of localized prostate cancer (PCa) and progression to castration-resistant prostate cancer (CRPC) (1–3). Despite androgen-ablation therapies, CRPC invariably develops due to aberrant reactivation of AR signaling through several mechanisms, such as *AR* gene amplification, synthesis of AR splice variants (AR-Vs) proteins, AR cofactor alteration, post-transcriptional modulations to AR and selectively up-regulation of a set of M-phase cell-cycle genes including *UBE2C* by AR (4–7).

AR mainly contains four functional domains, which are the NH2-terminal domain (NTD) carrying ligand-independent activation function (AF-1), the DNA-binding domain (DBD), hinge region and ligand-binding domain (LBD) containing ligand-dependent activation function (AF-2). Upon ligand binding, AR is translocated into the nucleus and binds to DNA sequences at androgen response elements (AREs), where it modulates the transcription of AR target genes by recruiting the basic transcription machinery as well as a series of co-regulators, including coactivators/corepressors, chromatin remodeling and histone modifying complexes (8–10). Chromatin remodelers and histone modifications, such as acetylation, methylation, ubiquitination and phosphorylation, have been demonstrated to play crucial roles in modulation of gene transcription (11–13). AR, regulation of AR by co-regulators, and its downstream signaling play crucial roles in prostate cancer development and progression (7,14–16). Substantial studies are being invested to well understand the modulation of AR in PCa/CRPC.

The MLL1, a homologue of trithorax (trxG) from *Drosophila*, is a key component of SET1/MLL1 histone methyltransferase (HMTase) complex, which possesses histone 3 lysine 4 (H3K4) methyltransferase activity. MLL1 has been implicated in regulation of *Hox* gene expression, particularly in early hematopoiesis, and its disorder is associated with abnormal hematopoiesis and acute leukemogenesis (17). MLL1 is also characterized as a subunit of MLL1-WDR5 (MLL1-MOF) complex, which not only contains a set of conserved subunits (e.g. WDR5, Ash2L, Menin), but

*To whom correspondence should be addressed. Tel: +86 24 31939077; Fax: +86 24 31939077; Email: zhaoyue@mail.cmu.edu.cn

includes MOF, a member of the MYST family that specifically acetylates H4K16. This documents a functional connection between the MLL HMT and the MOF HAT activities (18). Recently, it has been demonstrated that WDR5 as a subunit of MLL1-WDR5 complex plays a role in integrating histone phosphorylation and methylation during androgen signaling and in prostate cancer (19). On the other hand, it has been indicated that MLL1 complex including ASH2L and Menin participates in enhancement of AR action and acts as a potential therapeutic target in CRPC (20). Taken together, these studies indicate that MLL complexes have crucial roles in localized PCa and CRPC. However, the biological functions of several uncharacterized proteins in MLL complexes remain unclear.

BPTF associated protein of 18 kDa (BAP18) is encoded by gene *chromosome 17 open reading frame 49* (*C17orf49*). BAP18 also named as MGC49942 is reported as a component of chromatin complexes such as the MLL1-WDR5 complexes (18) and NURF/BPTF (21). BAP18 carries a Swi3, Ada2, N-CoR, (TF)IIIB (SANT) domain, which usually occurs in chromatin remodeling complex. SANT domain has a central role in chromatin remodeling by function as a unique histone-interaction module that couples histone binding to enzyme catalysis (22,23). However, BAP18 is an uncharacterized protein, it still needs to further elucidate the detail molecular mechanism and functional analysis of BAP18 in transcriptional regulation.

In this study, we identified CG33695, a *Drosophila* homologue of BAP18, as a novel coactivator of AR using an experimental system in *Drosophila*. In cultured mammalian cells, we demonstrated that BAP18 functionally interacts with AR and enhances AR-induced transactivation. Moreover, depletion of BAP18 decreases mRNA expression of a subset of AR target genes, including *FASN*, *FKBP5*, *UBE2C*, *PSA*. We further observed that BAP18 facilitates the recruitment of several components of MLL1 complex that lead to subsequent the enhancement of H3K4me3 and H4K16ac levels at androgen-response elements (ARE) of AR target genes. We also described that knockdown of BAP18 expression markedly inhibits the proliferation of prostate cancer cells and suppresses the growth of 22RV1 xenografts in castrated mice. Finally, we demonstrated that BAP18 is highly expressed in human prostate cancer samples compared with that in benign prostate hyperplasia (BPH). Taken together, these data describe the role of BAP18 in modulation of AR action and its association with MLL1 complex together with AR, and thus implicates BAP18 in PCa proliferation and CRPC progression.

MATERIALS AND METHODS

Drosophila stocks and genetics

All *Drosophila* stocks were raised at 25°C on cornmeal sucrose-based media. Flies of similar age were used for all comparisons. A modified position effect variegation (PEV) carrying ARAF-1-mediated transactivation (ARAF-1-PEV model) was generated as previous reported (24–26). A *Drosophila CG33695* cDNA clone was produced by OPEN biosystems (Clone ID BS16752). Human *C17orf49* cDNA coding sequence was amplified by PCR using Human IMAGE cDNA Clones (Open Biosystems & GE Dharmacon, Accession BC040036). *UAS-c17orf49* and *UAS-CG33695* constructs were generated by cloning *C17orf49* or *CG33695* cDNAs inserted into pCaSpeR3 and were sent to EMBL Drosophila Injection Service for generation of transgenic flies. A FLAG tag was inserted at the N terminus of *CG33695* cDNA in pCaSpeR3 constructs. Two loss-of-function mutants of *CG33695* ($CG33695^{k07716/+}$ and $CG33695^{DG06604/+}$) were ordered from Bloomington *Drosophila* Stock Center. To examine the effect of *CG33695* on ARAF-1-PEV experimental models, the male hemizygous for mutants (gain or loss of function) were crossed to ARAF-1-PEV female. The non-*TM3* progeny possessing the mutant allele and mosaic red eye were harvested for determination the effects of mutants on ARAF-1-PEV.

Eye disc histology analysis and immunofluoresence of polytene chromosomes have been included in Supplementary Data.

Cell culture

HEK293 cells were grown in Dulbercco's modified Eagle's medium (DMEM) supplemented with 10% fetal bovine serum (FBS), 50 units/ml penicillin and 50 units/ml streptomycin at 37°C under 5% CO_2. 22Rv1 and LNCaP cells were grown in Roswell Park Memorial Institute (RPMI) medium 1640 supplemented with 10% FBS, and penicillin/streptomycin. Before Dihydrotestosterone (DHT) treatment, cells were cultured in phenol red-free medium containing 10% dextran charcoal-stripped FBS (CDFBS) for 48 h, and then treated with 10^{-8}M DHT or vehicle (EtOH).

Luciferase reporter assay

22Rv1 cells were co-transfected with AR (20 ng), ARE-tk-luc (200 ng), a control Renilla luciferase plasmid (pRL) (2 ng) and GFP-BAP18, two truncated mutants of BAP18 in the indicated amounts. At 4 h post-transfection, the cells were rinsed and incubated in RPMI 1640 containing 5% charcoal-stripped FBS and supplemented with EtOH or 10^{-8}M DHT. After an additional 24 h, the cells were harvested and assayed for luciferase activities by use of a dual-luciferase reporter assay system (Promega) as described previously (27). The similar luciferase assay experiments in cos-7 cells as above were performed with the different reporter plasmids (200 ng of MMTV-tk-luc, PSA-tk-luc or ARE-tk-luc) and co-regulators (200 ng of BAP18, MLL1, Ash2L or MOF) as indicated. A total of 2.5 μg of plasmid DNA per well was used and the total amounts of the transfected DNA were kept constant by adding pcDNA3 plasmid (28). The expression plasmids carrying MLL1 or Ash2L were obtained from ADDGENE company. FLAG-tagged MOF expression plasmid was generously provided by Dr Ronald C. Conaway (29).

RNA isolation, RT and quantitative real-time PCR (RT-PCR)

Total RNA was isolated using Trizol (TAKARA). cDNAs were reverse transcribed from total RNA (2 μg) using

PrimeScript™ RT-PCR Kit (TAKARA). Realtime polymerase chain reaction was performed using the SYBR Premix Ex Taq kit (TAKARA) on a Mx3000P instrument (Agilent StrataGene). The sequences of the forward and reverse primers were shown in Supplementary Table S1. Gene expression levels were calculated relative to GAPDH using Stratagene Mx3000P software. The results were from a single experiment that was representative of at least two independent experiments.

RNA-seq analysis, Differentially Expressed Genes and Bioinformatics Analysis

The detailed description of this section has been included in Supplementary Data.

siRNA transfection, lentiviral production and infection

siRNA control (siCtrl) and siRNA duplexes against the gene encoding BAP18 (siC17orf49, to make the meaning of BAP18 keep consistent, siBAP18 has been used in all text instead of siC17orf49) were transfected using jetPRIME transfection reagent (Polyplus) following the manufacturer's instructions. Cells were analyzed 48 h after transfection to allow degradation of targeted mRNA. For lentiviral production and infection, control shRNA (shCtrl) lentivirus and shRNA against BAP18 (shBAP18) lentivirus targeting the same sequence as siBAP18#1 as above were purchased from Shanghai GeneChem Company. The sequences were listed in Supplementary Table S2.

Chromatin Immunoprecipitation (ChIP)

ChIP assays were performed according to previously described protocols (25). 22Rv1 cells were transfected with FLAG-BAP18 using jetPRIME transfection reagent (Polyplus) or infected with shBAP18, and then cultured for 2 days in phenol red-free RPMI 1640 supplemented with 10% charcoal-dextran-stripped FBS. At ∼90% confluency, cells were treated with 10^{-8}M DHT or EtOH for 12 h and harvested for ChIP. Immunoprecipitation of sonicated chromatin solutions was conducted by overnight incubation at 4°C with anti-AR (Thermo), anti-BAP18, anti-MLL1, anti-hMOF, anti-Ash2L, anti-H3K27me3 (Abcam), anti-H3K4me3 (Abcam) or anti-H4K16ac (Millipore) antibody. Cross-linking was reversed at 65°C, and DNA fragments were extracted with phenol-chloroform and precipitated with ethanol. The purified DNA was dissolved in TE buffer and analyzed by regular PCR. Primer sequences of PSA-ARE I/II were as follows: forward 5′-GCCAAGACATCTATTTCAGGAGC-3′, and reverse 5′-CCCACACCCAGAGCTGTGGAAGG-3′. DNA fragments was analyzed by real-time PCR (RT-PCR) with SYBR Green dye. Results were expressed as percentage of input chromatin and were derived from a single experiment that is representative of at least two independent experiments.

ChIP Re-ChIP

ChIP Re-ChIP analysis was performed in 22Rv1 cells as described previously (28). Protein–DNA complexes eluted from the first Immunoprecipitation (IP) were incubated with 10 mM DTT at 37°C for 30 min and diluted 1:50 in dilution buffer (1% Triton X-100, 2 mM EDTA, 150 mM NaCl, 20 mM Tris-HCl at pH 8.1) followed by Re-ChIP with the antibodies as indicated.

Cell growth, morphology and colony formation assay

22Rv1 cells were incubated for varying time periods, then harvested and stained with trypan blue, and viable cells were counted using a hematocytometer and plotted as a function of time. Different cells were visualized under a microscope to examine their morphologies. Single-cell suspensions were plated out at 100 cells per 3.5 cm dish in triplicate. Cells were then incubated for 7 days with or without DHT. Eventually, the medium was aspirated and dishes were fixed in methanol and stained with 3% Giemsa for 20 min, then rinsed and air-dried.

Xenograft tumor growth

All animal experiments were performed by the Institutional Animal Care and Use Committee of the China Medical University. 22Rv1 cells stably expressing shCtrl or shBAP18 were suspended in 100 μl medium with half Metrigel (BD Biosciences) and were injected (5.0×10^6 cells/mouse) subcutaneously into 5-week-old NOD/SCID mice (Vital River Laboratories). Mice were monitored every other day for tumor development. Tumor size was measured using an electronic caliper, and the tumor volume was determined with the formula: $V = (\pi/6) \times (L \times W)^{3/2}$, where V, volume ($mm^3$); L, biggest diameter (mm); W, smallest diameter (mm) (30). Eight weeks after inoculation, mice were killed in keeping with the policy of the humane treatment of tumor-bearing animals. Animal work was carried out in compliance with the ethical regulations approved by the Animal Ethics Committee of China Medical University.

Patients

Human prostate cancer tissues and benign prostatic hyperplasia tissues were obtained from 11 patients undergoing radical prostatectomy at the First Hospital of China Medical University. All samples were obtained with patients' informed consents.

Immunohistochemistry

Sections of prostate tissue specimens were prepared from clinical prostatectomy specimens in the First Hospital of China Medical University. The procedure was performed as previously described (28,31). Tissue sections of formalin-fixed, paraffin embedded tissue blocks were dewaxed in xylene, rehydrated in decreasing concentrations of ethanol, and blocked for endogenous peroxidase activity using 3% hydrogen peroxide. Antigen retrieval was carried out in citrate buffer (pH 6.0) at 130°C for 2 min. Then, non-specific antibody binding was blocked by incubating with goat serum for 15 min at room temperature. Slides were incubated with anti-BAP18 (1:100) overnight at 4°C. After washing, slides were incubated with biotinylated goat

anti-rabbit/mouse immunoglobulin, followed by incubation with avidin DH-biotinylated horseradish peroxidase complex (UltraSensitiveTM SP(Mouse/Rabbit)IHC Kit, Maixin Bio). The sections were developed with the diaminobenzidine substrate kit (Maixin Bio) and counterstained with hematoxylin. Images were taken with an Olympus microscope. This study was approved by the Ethics Committee of the Medical Faculty of the China Medical University.

Statistics

All statistical analysis was performed using the Statistical Product and Service Solutions (SPSS) (19.0) statistical software program. Student's two-tailed *t*-test was used for the determination of statistical relevance between groups. For analysis of clinical specimens, Mann–Whitney U test was used. *P*-values of $^{*}P < 0.05$; $^{**}P < 0.01$; and $^{***}P < 0.001$ were considered statistically significant.

RESULTS

Identification of CG33695 as a coactivator of AR in *Drosophila* experimental system

Numerous studies have shown that co-regulators of AR play a significant role in AR-mediated transactivation, and exert their crucial biological functions (4,32). Using a ARAF-1 associated PEV (ARAF-1-PEV model) in *Drosophila* experimental system, we have previously isolated several known proteins and clarified their novel functions as AR co-regulators involved in modulating AR actions via the different molecular mechanisms (24,28). In this system, the activation function-1 domain of AR (ARAF-1) carrying 1–720aa of AR is expressed driven by *GMR-Gal4* driver in the *Drosophila* eye. A reporter plasmid, which contains a gene encoding the green fluorescent protein (GFP) controlled by eight androgen response elements (AREs), was inserted into a pericentric region (80C2, C3L) (24,25,28). ARAF-1-induced transacivation can be assessed by the intensity of GFP expression in ARAF-1 PEV system. Interestingly, in this study, we isolated and identified an uncharacterized protein, CG33695 involved in regulating ARAF-1-induced transcriptional activity in *Drosophila*. Our results demonstrated that two loss-of-function mutants of *CG33695* ($CG33695^{K07716}$, $CG33695^{DG06604}$) individually decreased ARAF-1-mediated transactivation on GFP reporter expression system, indicating that CG33695 is a coactivator of AR in fly. To confirm this result, we constructed expression plasmids for *CG33695* (*UAS-CG33695*) and *C17orf49* (*UAS-C17orf49*), which is the human homologue of *CG33695* to generate the transgenic flies. As shown in Figure 1A, we observed that ectopic expression of *CG33695* or *C17orf49* enhances GFP transactivation by ARAF-1 in the eye discs (Figure 1A).

We further examine the localization of CG33695 on polytene chromosome using immunostaining. Our results demonstrated that CG33695 accumulated on many sites of euchromatic regions on polytene chromosomes, and CG33695 partially co-localized with dCBP, which was used as a positive control of AR coactivator in the euchromatic area (Figure 1B–E), suggesting that CG33695 may participate in active transcription on euchromatic region.

Using the National Center for Biotechnology Information database, multiple sequence alignments of the four species demonstrated that BAP18 among the four species displayed an overall high degree of homology in length and sequence (Figure 1F). BAP18s from the four species contain a conserved SANT domain, which occurs in chromatin associated proteins or transcriptional cofactors. Taken together, these results suggest that CG33695 acts as a coactivator of AR, and mainly accumulates in active transcription regions in *Drosophila*.

BAP18 physically interacts with AR *in vivo*

To study the effect of human homologue of CG33695 (BAP18) on AR-induced transactivation in human, we generated expression plasmid encoding FLAG-tagged BAP18, GFP-tagged BAP18 full length (BAP18-FL) and BAP18 truncated mutants carrying N terminal fragment (BAP18-N) or C terminus (BAP18-C) (Figure 2A), and performed a series of experiments in mammalian cells. We first test the interaction between BAP18 and AR by co-immunoprecipitation (Co-IP) experiments, HEK293 cells were co-transfected with AR and FLAG-tagged BAP18 expression plasmids. Precipitated proteins were detected by Western blotting using the antibodies as indicated. Our results showed that AR was precipitated with FLAG-tagged BAP18, and the interaction between AR and BAP18 was stronger in the presence of AR ligand (DHT) (Figure 2B). Then the similar Co-IP experiments were performed in PCa 22Rv1 cells, the results were in agreement with that in HEK293 cells, indicating that AR associates with BAP18 in 22Rv1 cells (Figure 2C). We then sought to identify the interaction domains in BAP18, to this end, HEK293 cells were co-transfected with expression plasmids encoding AR, GFP-tagged BAP18-FL and its truncated mutants (BAP18-N, BAP18-C) for co-IP (Figure 2D). The results demonstrated that AR individually interacts with BAP18 full length (FL), BAP18-N comprising 1–86aa or BAP18-C comprising 87–172aa, indicating that BAP18-N or BAP18-C mediates AR association with BAP18. To examine what is the role of SANT domain in MLL1 complex interaction, co-IP experiments using BAP18-FL and BAP18-C with SANT domain deletion were performed. As shown in Supplementary Figure S4, our data showed that there is no obvious difference between the interaction of BAP18-FL-MLL1 complex and BAP18-C-MLL1 complex, indicating that N-terminus carrying SANT domain may not be required for the association of BAP18 and MLL1 complex. These results suggest that N-terminus of BAP18 is required for its function in regulating AR action, but it is not required for AR and MLL1 complex interaction. Moreover, the results of immunofluoresence experiments showed that BAP18 was located in the nucleus with or without the treatment of DHT, and BAP18 were distributed together with AR in the nucleus with the treatment of DHT (Figure 2E). In addition, we examined the association of BAP18 and endogenous AR in PCa 22Rv1 cells, the data showed that BAP18 and AR were distributed in 22Rv1 cells in the presence or absence of DHT. Interestingly, BAP18-N was

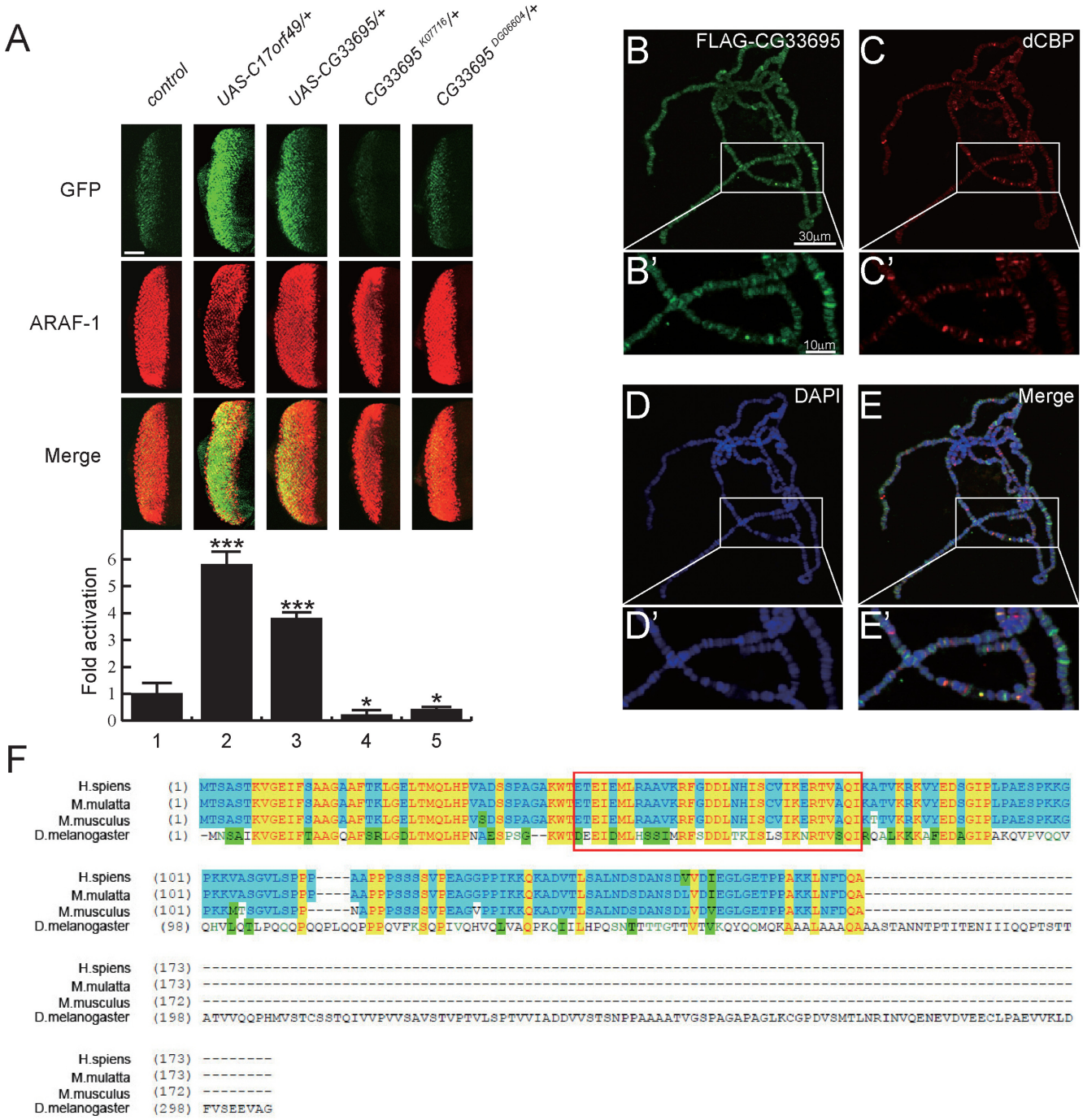

Figure 1. BAP18 enhances AR-induced transactivation in *Drosophila.* (**A**) Expression ARAF-1 in third instar eye imaginal discs driven by *GMR-GAL4* driver and carrying an *ARE-GFP* reporter in pericentric heterochromatin were crossed with lines harboring gain of function (*UAS-C17orf49*, *UAS-FLAG-CG33695*) or *CG33695* loss of function (*BL10680*, *BL21629*) mutants as indicated. The effect of BAP18 over-expression and mutations on ARAF-1 induced transactivation was evaluated by levels of GFP expression (upper panels). *GMR-GAL4* expressed ARAF-1 was detected with anti-AR (N-20) antibody (middle panels) and merged images are shown in the lower panel. Quantification of GFP expression revealed by color intensity is shown at the bottom. $*P < 0.05$, $***P < 0.001$. Scale bars, 50 μm. (**B**–**E**) Polytene chromosomes from the third instar larvae of flies carrying *UAS-FLAG-CG33695* and *GMR-GAL4* expression plasmids were dissected. The location of CG33695 on chromosomes was examined with anti-FLAG antibody (B and B′). Polytene were stained with anti-dCBP (C and C′) and with DAPI to visualize DNA (D and D′). E and E′, merged images. (**F**) Multiple-sequence alignments of the BAP18 from different species. The amino acid sequences of BAP18 in various species were extracted from the NCBI website. Multiple sequence alignments were performed using Vector NTI software (Life Technologies). Residues identical in all four species are highlighted in yellow; residues conserved are highlighted in blue; residues that are conserved but not identical are highlighted in green. Residues identical in the four species are highlighted in yellow; residues identical in *Homo sapiens* and *Mus musculus* are highlighted in blue; residues that are conserved but not identical are highlighted in green. *Drosophila melanogaster* CG33695 and *Human sapiens* BAP18 share 58% similarity. *Human sapiens* and *Macaca mulatta* BAP18 share 99%, while *Human sapiens* and *Mus musculus* BAP18 share 95% similarity. The red frame indicates the SANT domain. EMBL/RefSeq accession numbers are as follows: *Homo sapiens* (NP_777553.1), *Macaca mulatta* (AFE65909.1), *Mus musculus* (NP_665701.1) and *Drosophila melanogaster* (NP_001027248.1).

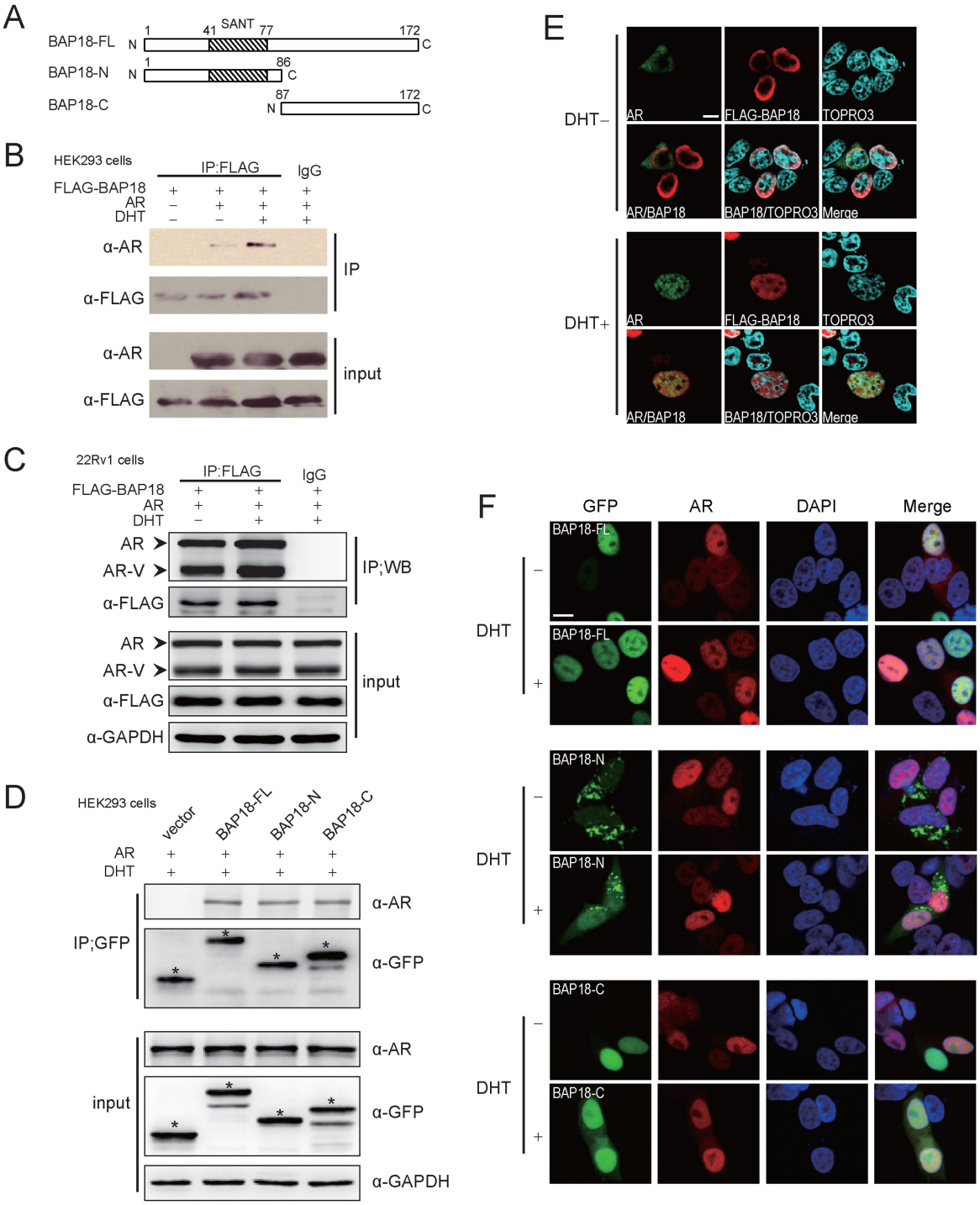

Figure 2. BAP18 interacts with AR *in vivo*. (**A**) Schematic diagram of full-length BAP18 and BAP18 truncation mutants used in this study. Numbers indicate amino acid position. (**B**) Co-immunoprecipitation (Co-IP) assay showing the interaction between BAP18 and AR *in vivo*. HEK293 cells were transfected with FLAG-BAP18 and AR expression plasmids with or without DHT (10^{-8} M). After 48 h, cell lysates were immunoprecipitated with anti-FLAG antibody or with IgG as a control. Precipitated proteins were examined by Western blotting using antibodies against FLAG or AR. Input represents 5% of the total cell extract used for each immunoprecipitation. (**C**) BAP18 interacts with AR and N-terminal AR variants in 22Rv1 cells. Cell lysates of 22Rv1 cells under the same transfection condition were subjected to Co-IP probed with FLAG antibody or IgG. (**D**) HEK293 cells were co-transfected with GFP-BAP18 or a series of GFP-BAP18 mutation expression plasmids and AR as indicated with or without DHT (10^{-8} M) for 48 h. IP performed using anti-GFP and whole-cell extracts (input) were analyzed by immunoblotting using the indicated antibodies. (**E**) HEK293 cells were co-transfected with FLAG-BAP18 expression plasmids and AR and treated with or without DHT (10^{-8} M). Then cells were stained with TOPRO3 to visualize the nucleus (blue), anti-FLAG (red), anti-AR (green). The localization of the two proteins was analyzed by a fluorescence microscope. Scale bars, 50 μm. (**F**) 22Rv1 cells were transfected with plasmids expressing for GFP-BAP18 or two truncated mutants and treated with or without DHT (10^{-8} M). The endogenous AR were immunostained with anti-AR (red), whereas BAP18 and two truncates localizations were detected by direct GFP fluorescence. Blue is the DAPI stain of the nucleus. Scale bars, 10 μm.

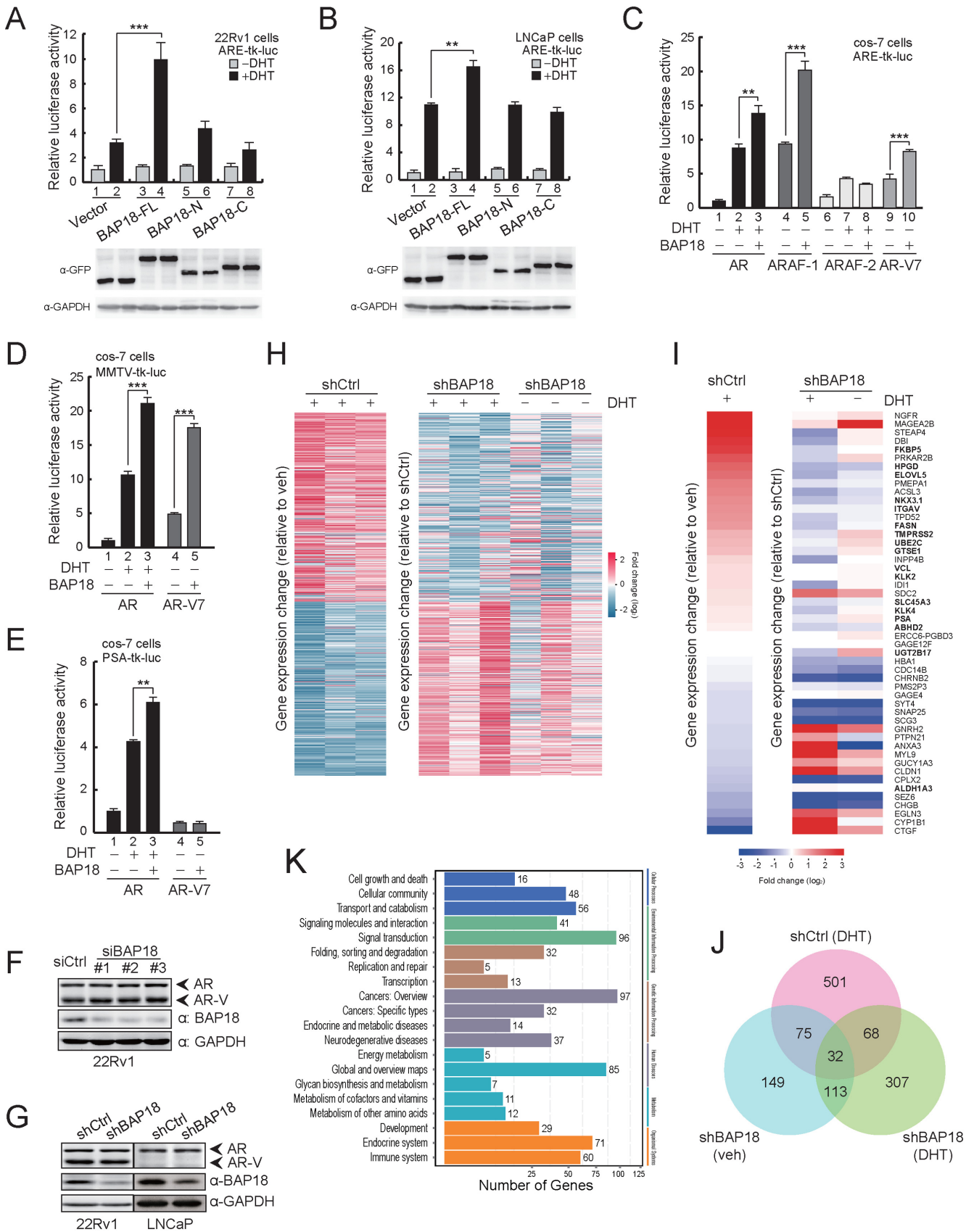

Figure 3. BAP18 enhances AR-induced transactivation and knockdown BAP18 inhibits AR target gene expression. (**A–B**) The transcriptional activity of AR was increased by overexpression of BAP18 both in 22Rv1 and LNCaP cells. Cells were transfected with full length BAP18 or its truncated mutants as

partially localized in the cytoplasm, while BAP18-C was still distributed in the nucleus, suggesting that the nuclear localization signals (NLSs) were mainly located in the C-terminus of BAP18 (Figure 2F). Collectively, these data indicated that BAP18 physically associates with AR in mammalian cells.

BAP18 up-regulates AR-mediated transactivation in mammalian cells

To explore whether BAP18 is able to enhance AR action in mammalian cells, we first performed luciferase assay in PCa 22Rv1 cells and LNCaP cells. The cells were co-transfected with pGL3-ARE-tk-luc reporter vector together with AR expression plasmid alone, or together with the expression plasmids encoding BAP18 full length (BAP18-FL) or its truncated mutants (BAP18-N and BAP18-C) with or without the treatment of DHT (Figure 3A and B). Our results demonstrated that BAP18-FL significantly enhanced AR-mediated transactivation in the presence of DHT, while BAP18-N or BAP18-C has no obvious effect on it. These results suggest that BAP18 co-activates AR-mediated transactivation in a ligand-dependent manner, and the entire BAP18 is required for its coactivator function. Then, we further examined the effects of BAP18 on the transactivation mediated by artificially truncated AR, including ARAF-1 containing ligand-independent domain and ARAF-2 comprising ligand-dependent domain. The results showed that BAP18 significantly increased ARAF-1-induced transactivation in the absence of DHT, which is a little stronger than that on AR full length with the treatment of DHT. However, we have not detected the obvious effect of BAP18 on ARAF-2 even in the presence of DHT (Figure 3C lane 1–8). To confirm these results, we turn to examine the effect of BAP18 on AR variant (AR-V7) with pGL3-ARE-tk-luc, MMTV-tk-luc or PSA-tk-luc reporters. AR-V7 is lack of C-terminal ligand-binding domain and constitutively active to be resistant to traditional androgen deprivation therapy in PCa. Our results demonstrated that BAP18 dominantly up-regulated AR-V7-mediated transcriptional activity in the absence of DHT (Figure 3C lane 9–10, Figure 3D–E). These results indicated that BAP18 functions as a coactivator of AR in mammalian cells, and specifically enhances truncated ARAF-1 or N-terminal variant of AR (AR-V7) action in the absence of DHT.

We next examined whether BAP18 is required for regulating the endogenous AR target genes. To this end, we turn to LNCaP cells, in which AR is constitutively expressed, and 22Rv1 cells harboring coexpression of AR full length and AR variants (AR-Vs) and analyze the expression of AR target genes with the depletion of BAP18. Three kinds of siRNAs against BAP18 (siBAP18 #1, #2, #3) were individually transfected into 22Rv1 cells and an 80% reduction of BAP18 expression was detected for each of them by Western blotting (Figure 3F). We thus selected siBAP18#1 to produce shRNA retrovirus against BAP18 (shBAP18) in 22Rv1 cells and LNCaP cells, as shown in Figure 3G, an 80% reduction of BAP18 expression by shBAP18 in 22Rv1 and a 75% reduction of BAP18 in LNCaP cells were confirmed by Western blotting experiments (Figure 3G). BAP18 mRNA level (*C17orf49*) reduced by shBAP18 was examined by q-PCR experiments (see Supplementary Figure S1A–B).

To systematically investigate the epigenome-wide impact of BAP18 on global AR-mediated gene regulation, we contucted knockdown experiments to perform mRNA expression analysis coupled with high throughout sequencing (RNA-seq analysis). From the gene expression data, we identified 609 differentially expressed genes (DEGs) after treatment with synthetic androgen (DHT) in 22Rv1 cells. These genes were then partially regulated by siRNA against the gene encoding BAP18 (Figure 3H). The DEGs were listed in Supplementary Table S3. Knockdown of BAP18 obviously modulated the expression of genes induced by DHT treatment, suggesting that BAP18 is genomically involved in modulation of AR-driven transcription. To assess whether the modulation function of BAP18 on various genes in the presence of DHT is similar with that in the absence of DHT, we compared the RNA-seq analysis data obtained from 22Rv1 cells carrying shBAP18 treated with or without DHT and observed partial overlap in AR target gene regulation (Figure 3I). Venn diagram showed that expression of 107 and 100 AR-driven genes was modulated by shBAP18 in the absence or presence of DHT, respectively. The number of androgen-induced genes with altered expression was 32 in shBAP18 cells in both presence and absence of DHT. The overlap between all three circles indicates that these genes activated by AR and AR variants may be regulated by BAP18 (Figure 3J). We then examined cellular processes in which these diferentially expressed genes are mainly involved by performing the enrichment analysis of KEGG pathway (Figure 3K, Supplementary Figure S2). The results demonstrated that the DEGs are mainly involved in cellular processes, human diseases, as well as organismal systems.

←

indicated in the absence or presence of ligand (DHT). BAP18 enhances AR mediated transactivation, and both of N- terminus and C-terminus are required for its function. The expression levels of BAP18 truncated mutations were detected by Western blotting. (**C**) BAP18 enhances AR, ARAF-1 or AR-V7 mediated transactivation. The plasmids expressing the full-length or truncated AR were transfected into cos-7 cells with or without FLAG-BAP18, and the cells were treated with or without DHT (10^{-8}M). After 24 h of DHT, cell lysates were subjected to luciferase assay. Relative luciferase units shown are the mean value at least three times. (**D**) BAP18 enhances AR or AR-V7-induced tranasactivation on MMTV-tk-luc reporter. Cos-7 cells were co-transfected with MMTV-tk-luc and pRL-TK together with the indicated expression plasmids with or without DHT (10^{-8}M). (**E**) BAP18 enhances AR or AR-V7-induced tranasactivation on PSA-tk-luc reporter. The similar luciferase assays were performed as above with PSA-tk-luc in cos-7 cells. (**F**) 22Rv1 cells were harvested 48 h after transfection with three different siRNAs (#1, #2 and #3) targeting BAP18 or control siRNA (siCtrl). The expression of BAP18 was measured by Western blotting with anti-BAP18 antibodies. (**G**) 22Rv1 and LNCaP cells were infected with shRNA Lentivirus against BAP18 (shBAP18) or shRNA Lentivirus control (shCtrl). Western blotting analysis data are shown. (**H**) RNA-seq analysis profile of shBAP18 or shCtrl after treatment with or without DHT in 22Rv1 cells. Heat map displays the altered expression of DHT-induced genes upon BAP18 knockdown. Fold change is indicated at right. (**I**) Heat map representation of BAP18 knockdown on the expression of various genes in the absence or presence of DHT. Bold letters, widely studied AR target genes. (**J**) Venn diagram showing DHT-regulated genes in shCtrl and shBAP18 cells in the presence of DHT or vehicle. (**K**) Biological processes of DHT-induced transcripts in shCtrl and shBAP18 cells as revealed by KEGG pathway analysis.

Next, using quantitative PCR (qPCR), we assessed the role of BAP18 in AR signaling. Similar to what we observed in luciferase assay and RNA-seq analysis, BAP18 depletion resulted in a significant ($P < 0.05$ or $P < 0.01$) decrease in the DHT-mediated expression of 12 AR target genes, including *PSA*, *HPGD*, *ELOVL5*, *ITGAV*, *KLK2*, *KLK4*, *ALDH1A3*, *FKBP5*, *UBE2C*, *SLC45A3*, *FASN* and *VCL* in 22Rv1 cells (Figure 4A). While knockdown of BAP18 decreased the induction folds of *PSA*, *HPGD*, *ELOVL5*, *ITGAV*, *KLK2*, *KLK4*, *ALDH1A3*, *FKBP5*, *UBE2C*, *SLC45A3*, *FASN*, *GTSE1*, *UGT2B17* and *VCL* expression by DHT in LNCaP cells (Figure 4B). Taken together, our results indicate that BAP18 co-activates AR or AR variant-mediated transactivation and knockdown of BAP18 reduced a subset of endogenous AR target genes transcription *in vivo*.

BAP18 facilitates the recruitment of MLL1 associated proteins to the promoters of AR target genes

It has been shown that MLL1 complex, which is involved in the methylation of histone H3 at lysine 4 and the acetylation of histone H4 at lysine 16, is implicated in epigenetic transcriptional activation (18). MLL1 associated complex has also been proved to participate in modulating AR signaling (19,33). Having established that BAP18/MGC49942 is an uncharacterized component of MLL1 complex (18), and BAP18 is involved in up-regulation of AR action in this study. However, the molecular mechanisms and biological functions of BAP18 are largely unknown. We thus tested whether BAP18 was recruited to AREs of its target genes together with MLL1 associated proteins, and how the depletion of BAP18 influenced the level of histone modifications on the promoter region of AR target genes. ChIP assays were performed in 22Rv1 cells with ectopic expression of BAP18 in the presence or absence of ligand (DHT) using the antibodies as indicated. The results showed that BAP18 or AR was recruited to the promoter region of *PSA* gene (PSA-ARE I/II) upon DHT induction. Interestingly, the recruitment of AR to PSA-ARE I/II was also promoted by ectopic expression of BAP18. Meanwhile, the methylation levels of histone H3K4me3 and acetylation of histone H4K16ac on PSA-ARE I/II region were significantly enhanced by BAP18, but methylation of histone H3K27me3 was not remarkably influenced by BAP18 (Figure 4C and Supplementary Figure S3A). In order to confirm these results, we performed the similar ChIP assays with knockdown of BAP18, in agreement with the above results, our data showed that the recruitment of AR was diminished by knockdown expression of BAP18, the levels of H3K4me3 and H4K16ac were decreased by shBAP18 in the presence of DHT. Moreover, as shown in Figure 4D, our results demonstrated that knockdown of BAP18 prominently attenuated the recruitment of MLL1 associated proteins, including MLL1, Ash2L and MOF to PSA-ARE I/II region with or without DHT stimulation (Figure 4D and Supplementary Figure S3B). Furthermore, to assess whether BAP18 is recruited to the promoter of AR target gene together with AR, MLL1, or MOF, ChIP re-ChIP experiments were performed. ChIP assays were first performed with antibodies against AR or BAP18 in the soluble chromatin isolated from 22Rv1 cells in the absence or presence of DHT, the precipitates from ChIP were subjected to re-ChIP with antibody against the second protein as indicated. The results showed that BAP18 occupied androgen response element is simultaneously bound by AR, MLL1 or MOF (Figure 5A). Collectively, these results suggest that BAP18 can be recruited to the promoter of AR target genes, and facilitates the recruitment of MLL1 associated proteins or AR itself to the promoters of AR target genes.

Having demonstrated the recruitment of BAP18 and MLL1 associated proteins to AR-bound chromatin regions, we then set out to investigate whether BAP18 is able to interact with MLL1 associated proteins together with AR in PCa cells. As expected, the results of co-IP experiments demonstrated that AR interacts with BAP18 and MLL1 associated proteins, including MLL1, Ash2L, MOF and Menin with or without DHT treatment. Interestingly, knockdown of BAP18 did not alter the interactions between MLL1, Ash2L and Menin with AR in the presence or absence of DHT. Whereas when BAP18 was depleted by shBAP18, the association of MOF with AR was decreased, indicated that BAP18 may act as a scaffolding protein for facilitating the association between MOF and AR (Figure 5B). In LNCaP cells, in agreement with that in 22Rv1 cells, the results showed that BAP18 associated with AR and MLL1 complex, moreover, depletion of BAP18 attenuated the association between AR and MOF (Figure 5C–D). In addition, luciferase assays were performed to examine the effects of subunits of MLL1 complex on AR action, our results demonstrated that BAP18, MLL1 or Ash2L enhanced AR-induced transactivation in cells. BAP18/MLL1 or BAP18/Ash2L additively enhanced AR-dependent transactivation. Unexpectedly we did not observe the obviously effect of MOF itself on modulation of AR action (Figure 5E). Taken together, our results suggest that BAP18 and MLL1 complex may function together with AR to regulate AR-mediated transactivation.

BAP18 is required for tumor growth and proliferation in prostate cancer

AR signaling plays a critical role in prostate cancer and the progression of CRPC (33,34). Having demonstrated that BAP18 is involved in modulation of AR-induced transactivation, and knockdown of BAP18 results in a significant decrease in the expression of AR target genes, such as *PSA*, *KLK4*, *UBE2C*, *SLC45A3* and *FASN*, which were tightly associated with prostate cancer growth or CRPC progression. We then set out to investigate the biological role of BAP18 in PCa cells, we examined the effect of BAP18 on the growth and proliferation of PCa cells with shRNA against BAP18 in 22Rv1 cells. Growth curves analysis at 0, 2, 4, 6 and 8 days showed that depletion of BAP18 attenuated cell proliferation in the presence or absence of DHT (Figure 6A). Consistently, colony formation experiments demonstrated that knockdown of BAP18 formed lower number of colonies than that of control in a DHT-independent manner (Figure 6B). In addition, microscopic observation also indicated that BAP18 knockdown suppressed the cell growth in 22Rv1 or LNCaP cells (Supplementary Figure S5A–B). We then ask whether the function of BAP18 on cell growth

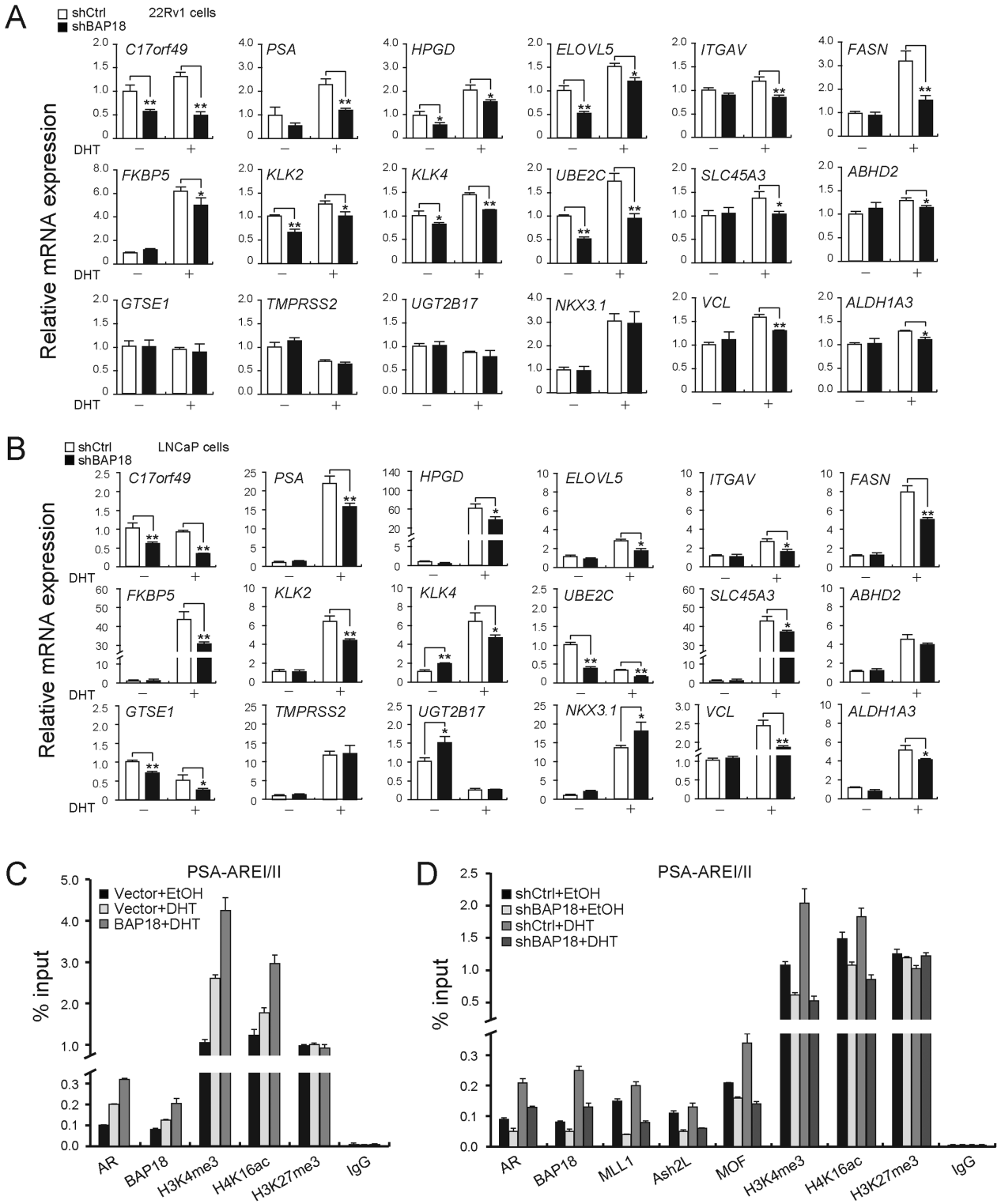

Figure 4. BAP18 facilitates the recruitment of MLL1 subcomplex to the promoters of AR target genes. (**A–B**) Real-time PCR (RT-PCR) analysis showing the effect of BAP18 knockdown on activation of 17 AR target genes. 22Rv1 or LNCaP cells with knocking down BAP18 expression by shBAP18 as indicated were harvest after treatment with or without DHT (10^{-8}M) for 24 h. Total RNA was analyzed by Real-time quantitative PCR (RT-qPCR). Levels of all mRNAs were normalized to that of GAPDH mRNA. Statistical significance of differences between experimental groups was assessed *t*-test. Error bars represent mean ± SD. $*P < 0.05$; $**P < 0.01$; and $***P < 0.001$. (**C**) 22Rv1 cells were transfected with FLAG-BAP18 for 40 h and treated with DHT (10^{-8}M) for an additional 8 h and subjected to ChIP assay using antibodies specific to AR, BAP18, MOF, H4K16ac, H3K4me3 and H3K27me3. The immunoprecipitated DNA fragments were PCR amplified using primers flanking the promoter region of *PSA* gene (PSA-ARE I/II). (**D**) ChIP assay were performed using indicated antibodies in 22Rv1 cells with knocking down BAP18 expression by shBAP18 with or without DHT (10^{-8}M) and analyzed by qPCR. The data are representative of more than two independent experiments.

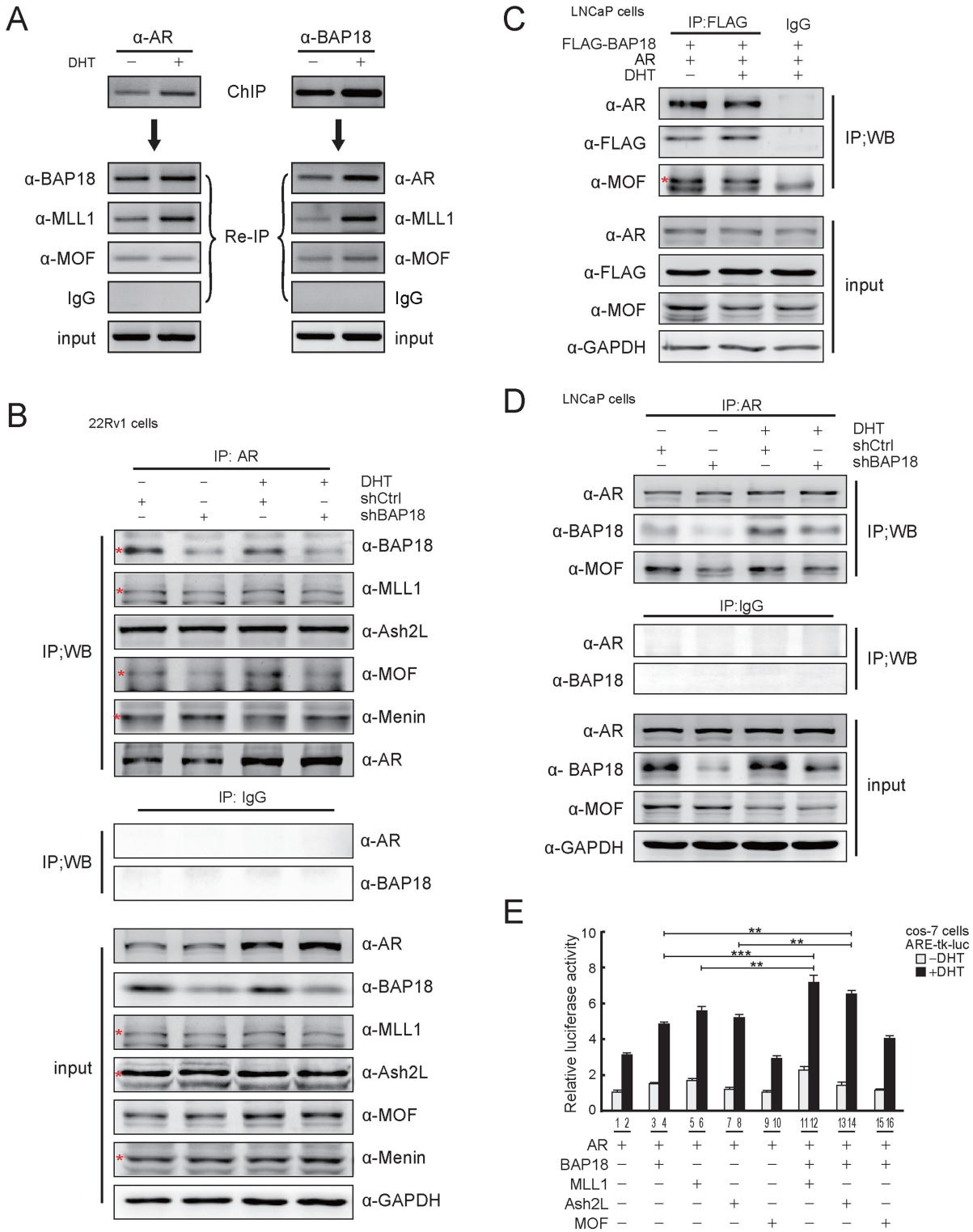

Figure 5. BAP18 interacts with MLL1 subcomplex. (**A**) BAP18, AR, MLL1 and MOF are recruited together to cis-regulatory elements of *PSA* in the absence or presence of DHT. ChIP/re-ChIP experiments were performed using specific antibodies against BAP18, AR, MLL1, MOF or IgG as indicated. DNA eluted from unprecipitated chromatin was used as input. Chromatin samples were analyzed by gel electrophoresis. (**B**) 22Rv1 cells were treated with shBAP18 or shCtrl, and immunoprecipitated using anti-AR antibodies or IgG. Precipitated protein complex were analyzed by Western blotting with antibodies as indicated. Input represents 5% of the total cell extract used for each immunoprecipitation. (**C** and **D**) LNCaP cells were incubated with or without DHT, transfected with BAP18 expression plasmids or siRNA against BAP18 (siBAP18). Immunoprecipitate generated with anti-FLAG or anti-AR antibody was subjected to Western blotting with the indicated antibodies. (**E**) AR-dependent transactivation requires BAP18, MLL1 or Ash2L in cells. Cos-7 cells were co-transfected with the AR together with BAP18, MLL1, Ash2L or MOF expression plasmid as indicated. The total amount of the transfected DNA was kept constant with the empty vector.

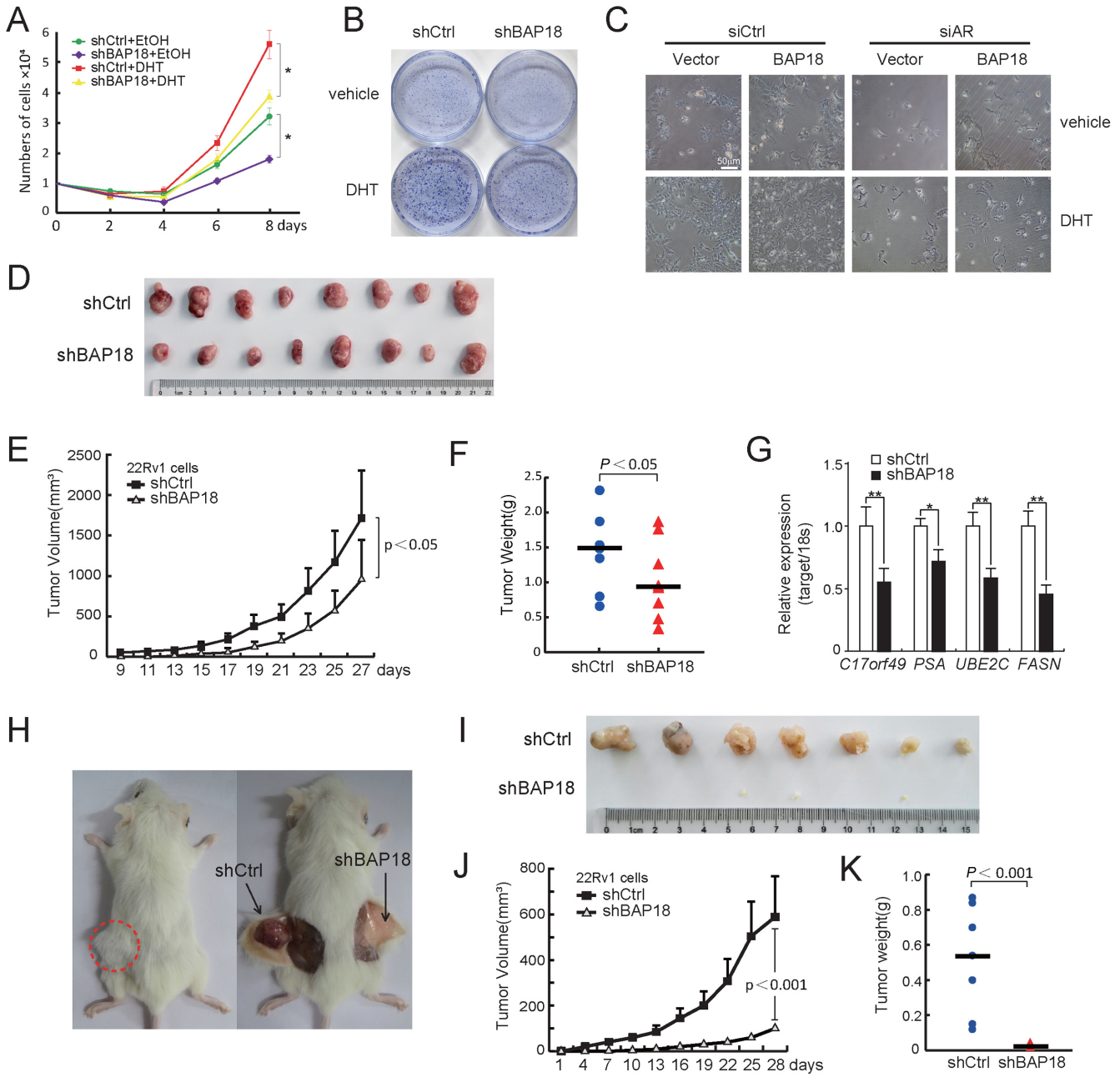

Figure 6. Knockdown of BAP18 inhibits tumor growth of prostate cancer xenograft. (**A**) Growth curve of the stable knockdown by shBAP18 in 22Rv1 cells. Total cell numbers were counted on days 0, 2, 4, 6 and 8. Data were means ± SD of three independent experiments performed in triplicates. *$P <$ 0.05. (**B**) Representative microphotographs of clone formation experiments of stable 22Rv1 cells. A total of 1×10^4 cells were seeded in 3.5-cm dishes for 7 days. Colonies were stained by crystal violet. (**C**) 22Rv1 cells were transfected with siAR or siCtrl for 4 h, then transfected with BAP18 overexpression plasmids or vector in the presence of DHT or not. At 72 h after transfection, microscopic analysis of the cells were performed. Scale bars, 50 μm. (**D**) Photograph showing the xenograft tumor in male SCID mice with shCtrl (left) or shBAP18 (right) stable 22Rv1 cells. Tumors were dissected from mice at the 28th day post injection. (**E–F**) Dissected tumors were measured. The average volumes or weights and standard errors were calculated for each group. *$P < 0.05$. (**G**) The mRNA samples from tumor xenograft mice were isolated, and qPCR for the indicated mRNA was performed. Data were expressed as means ± SD (n = 8). Statistical significance was determined using *t*-test, *$P < 0.05$, **$P < 0.01$. (**H–I**) Representative photograph showing the xenograft tumor in male SCID mice treated castration injected with shCtrl (left) or shBAP18 (right) stable 22Rv1 cells. (**J**) The average tumor volume of shCtrl and shBAP18 were plotted over days after tumor cell injected. Data points represent the mean of 14 tumors from 7 mice. Bars represent standard deviation of the mean, $P < 0.001$. (**K**) Four weeks later tumor weights were statistically analyzed using *t*-test, $P < 0.001$.

and proliferation of PCa cells is related to AR, to this end, we turned to 22Rv1 cells and performed the cell proliferation experiment with depletion of AR, our results showed that the cell proliferation promoted by ectopic expression BAP18 was significantly attenuated by downregulation of AR (Figure 6C). Efficiency of siRNA against AR or ectopic expression of BAP18 was shown in Supplementary Figure S6. These data suggested that the cell growth of PCa cells promoted by BAP18 is related to AR.

To further confirm these results, we examined the effects of BAP18 on prostate tumor growth *in vivo* using a mouse xenograft model. 22Rv1 cells infected with lentivirus carrying shBAP18 or shCtrl were separately injected into right (shBAP18) or left flanks (shCtrl) of 5-week-old male NOD/SCID mice (n = 8). Subsequently, the tumor volumes were measured every two-day after injection. Our data showed that the size of xenograft tumor from shBAP18-22Rv1 cells was smaller than that from shCtrl-22Rv1 cells (Figure 6D). The tumor volumes from shBAP18-22Rv1 cells demonstrated slower growth rate than those from the control cells (Figure 6E). After four weeks, the tumors were harvested and weighted. The average tumor weight from shBAP18-22Rv1 cells was lower than that from the control cells (Figure 6F). To further assess the influence of BAP18 on AR target gene expression using the above xenograft tumors in mice, total RNA was individually extracted from the xenograft tumors and qPCR was performed to analyze the gene expression of *C17orf49*, *PSA*, *UBE2C* and *FASN* (Figure 6G). In agreement with modulation of BAP18 on AR target genes in PCa 22Rv1 cells as shown in Figure 4A, our results showed that BAP18 knockdown resulted in significant decreases in a subset of AR target gene expression in xenograft tumor in mice.

Having identified that BAP18 is a coactivator of AR-mediated transcription, and up-regulates the expression of a series of putative AR target genes, including *UBE2C* and *FASN* genes, which play important roles in CRPC progression (4,35,36). We also found that BAP18 promotes PCa cell growth in the presence or absence DHT (Figure 6A and B, and Supplementary Figure S5A and B). We then set up to test whether BAP18 is necessary for PCa cell growth under androgen-depleted conditions. We implemented the castration operation in male NOD/SCID mice and then injected shBAP18-22Rv1 cells into right or shCtrl-22Rv1 cells into left flunks of the castrated mice (n = 8). The tumor volumes were measured every three days after injection. The results indicated that knockdown of BAP18 significantly suppressed xenograft tumor growth under androgen-depleted condition *in vivo* (Figure 6H–I). The tumor volumes from BAP18-depleted 22Rv1 cells showed much slower growth rate than those from shCtrl-22Rv1 cells (Figure 6J). After four weeks, the tumors were harvested and weighted. The average tumor weight from shBAP18-22Rv1 cells was much lower than that from control cells, indicating that knockdown of BAP18 remarkably reduces PCa cell growth in castrated mice (Figure 6K). Taken together, these data suggest that BAP18 plays an important role in PCa growth and proliferation, and BAP18 is required for PCa cell growth under androgen-depleted condition.

BAP18 is highly expressed in prostate cancer biopsies

The requirement for BAP18 in PCa cell growth and proliferation encouraged us to examine BAP18 expression in several PCa cell lines and clinical prostate tissues. As shown in Figure 7A, the expression of BAP18 were detected in AR-positive (22Rv1, LNCaP, VCaP) or AR-negative (DU145) PCa cell lines, indicating that BAP18 may play multiple roles in prostate cancer beyond AR. To detect the expression of BAP18 in clinical prostate samples, we collected nine clinical PCa and two BPH samples, Western blotting results showed that the expression of BAP18 protein was stronger in clinical PCa tissues than that in BPH tissues. RT-PCR results showed the expression of BAP18 mRNA (*C17orf49*) in clinical prostate tissues was in accordance with BAP18 protein expression (Figure7B and C). In addition, we examined the expression of BAP18 in clinical prostate biopsies including 92 cases of PCa and 33 cases of BPH using immunohistochemical (IHC) analysis. We found that PCa samples had strong staining for BAP18, whereas weak staining was observed in BPH. BAP18 was detected in the nucleus (Figure 7D). Semiquantitative analysis showed that BAP18 had obviously higher immunostaining in PCa samples than that in BPH. In PCa, BAP18 expression did not correlate with different Gleason Grades (Figure 7E). Among 33 benign prostate specimens, 13 displayed low staining for BAP18 (39.4%), 15 displayed middle staining (45.4%) and 5 displayed high staining (15.2%). Among 92 primary PCa specimens: 14 were low (15.2%); 23 were middle (25%); 55 were high (59.8%) (Figure 7F). Taken together, our data suggest the expression of BAP18 may be crucial for the prostate tumorigenesis.

DISCUSSION

BAP18 has been mentioned as an uncharacterized subunit of MLL1-MOF complex, which is involved in up-regulation of gene transcription. BAP18 is an 18 kDa protein that carries a SANT domain in its N-terminus. However, the role of BAP18 in modulating nuclear receptor-mediated transcription and the biological function of BAP18 are largely unknown. In this study, we identified CG33695 as a new coactivator of AR using an experimental screening system (ARAF-1-PEV model) in *Drosophilar* (24,25,28). BAP18 (MGC49942) encoded by gene *C17orf49* is a human homologue of CG33695. We demonstrate that BAP18 associates with AR, and enhances AR-induced transactivation in mammalian cells. In addition, its N-terminus containing SANT domain is required for co-activator function of BAP18, but not for its interaction with AR and MLL1 complex. Importantly, we provide the evidence that BAP18 forms a subcomplex with AR and MLL1 associated proteins. Meanwhile, BAP18 facilitates the recruitment of MLL1 subcomplex to AREs of AR target genes, thereby increasing histone H3K4me3 and H4K16ac levels for maintaining the active gene transcription. Moreover, we show that knockdown of BAP18 attenuates cell growth and proliferation of prostate cancer 22Rv1 cells even under androgen-depleted condition *in vivo*.

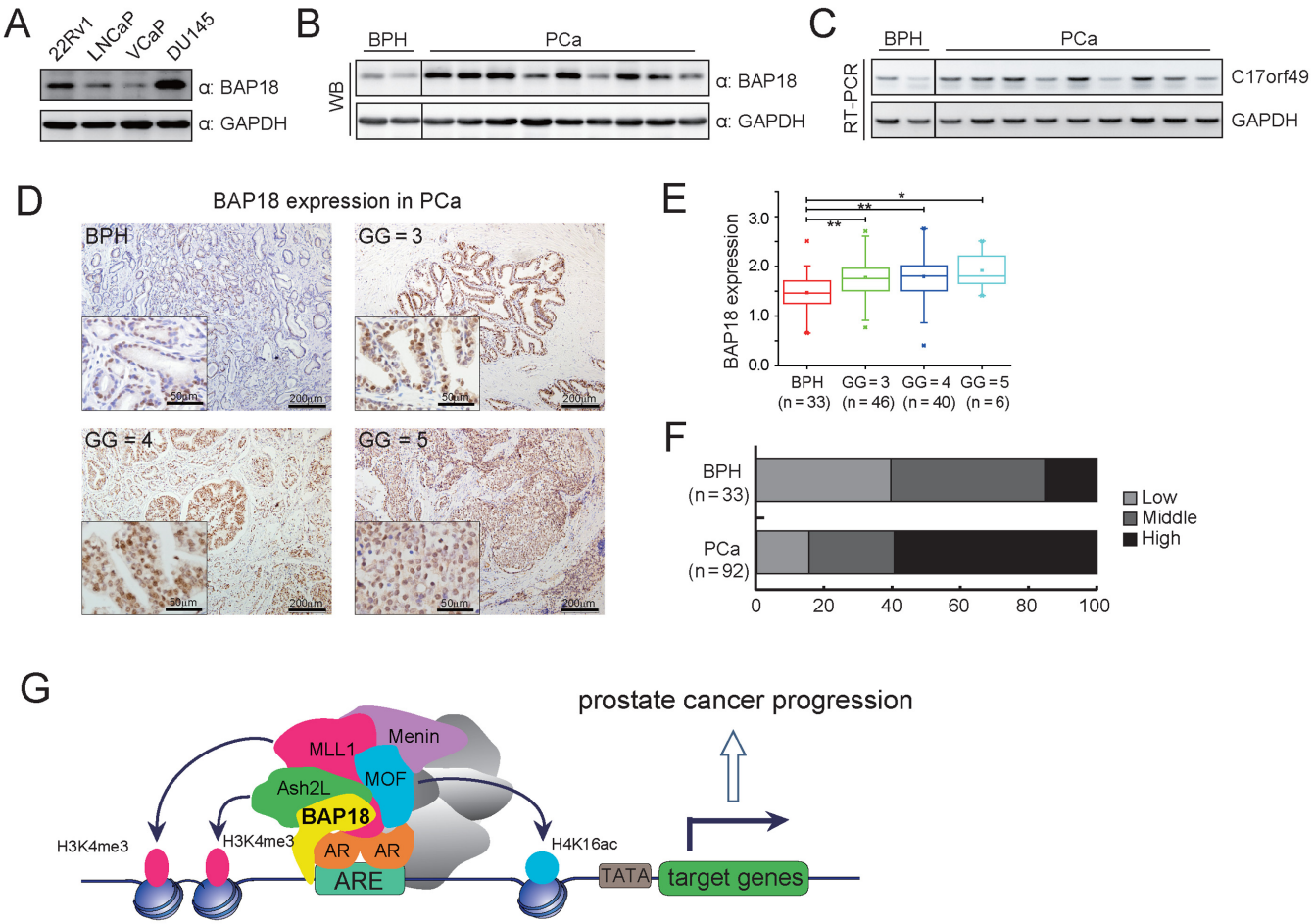

Figure 7. BAP18 mRNA and protein expression level in clinical prostatectomy specimens. (**A**) Expression of BAP18 in different prostate cancer cell lines. (**B** and **C**) All fresh tissue specimens were from patient undergoing radical prostatectomy without any hormonal therapy. Expression of BAP18 protein (B) and mRNA (*C17orf49*) (C) were detected in PCa or BPH. (**D**) Representative tissue stained with an antibody against BAP18. Stronger staining of BAP18 was seen in PCa (Gleason Grade [GG] 3, 4 and 5) than that in BPH (magnification 10x; Scale bars: 200 μm). Rectangle represents magnification image (magnification, 40x; scale bars: 50 μm). (**E**) BAP18 expression in PCa samples with different Gleason Grades (GG = 3, 4 and 5) compared with BPH (n = 33). BAP18 has obviously higher staining in PCa samples compared with that in BPH. In PCa, no significant correlation between the intensity of BAP18 immunostaining and different Gleason Grades could be observed. Statistical significance of the differences between experimental groups was assessed *u*-test, $*P < 0.05$, $**P < 0.01$. (**F**) Presentation for the percentage of PCa or BPH samples with low, middle or high expression of BAP18. (**G**) Schematic representation of the key role of BAP18 in up-regulation of AR-induced transactivation and promotion of prostate cancer progression.

BAP18, an uncharacterized subunit of MLL1-MOF complex, facilitates MLL1 subcomplex to the promoter of AR target gene

A complex containing MLL1 and MOF has been purified from a human cell line that stably expressed WDR5 protein. The purified complex possesses MLL1-mediated histone methyltransferase activity on histone H3K4 mono-, di- and trimethylation and MOF-mediated histone acetyltransferase activity on histone H4K16 acetylation. Both histone modifications are necessary for transcription activation on active genes. BAP18 (MGC49942) with unknown function has been detected in the MLL1-MOF complex (18). On the other hand, the screening of the H3K4me3 interactome with ChIP-Seq profiling revealed a large number of chromatin readers with unknown function. Among them, BAP18 is one of the candidates as the interactors of H3K4me3. BAP18 has been further purified as a part of NURF/BPTF complex (21). It has been also proved by structural evidence showing that DPY-30, a subunit of COMPASS-like complex interacts with BAP18 (37). It is tempting to speculate that BAP18 may be involved in transcription regulation. Here, our results from both screening with ARAF-1-PEV model and reporter assays suggest that CG33695/BAP18 participates in co-activating AR-mediated transactivation in *Drosophila* experimental model (Figure 1A) and mammalian cells (Figure 3A–C). Moreover, we detect that BAP18 associates with AR, and its N- terminus carrying SANT domian or C-terminus mediates the association between AR and BAP18 (Figure 2), while the entire of BAP18 is required for its regulation function for AR action (Figure 3A–B). These intriguing findings raise the following questions: what is the epigenetic mechanism for the role of BAP18 in modulation of AR-induced transcription, and whether a functional link may exist between BAP18 and histone modification or chromatin remodeling complex on the context of AR target genes. Our

study provides the evidence that BAP18 is recruited to the ARE together with AR (Figure 5A). We further demonstrate that BAP18 facilitates the recruitment of MLL1 subcomplex, including MLL1, MOF, Ash2L and Menin to ARE and thereby effecting trimethylation of histone H3K4 and acetylation of H4K16 (Figure 4C and D). In addition, BAP18 forms a complex together with MLL1 associated proteins (Figure 5). It has been indicated that WDR5, by virtue of its ability to associate with H3T11P facilitates the recruitment of MLL1 complex for histone H3K4 trimethylation leading to gene activation (19). Thus, our results show that beyond the roles of WDR5 and H3T11P in facilitating the recruitment of MLL complex to AR target genes, the association of BAP18 and AR in the MLL1 subcomplex provides an additional attractive mechanism by which BAP18 is required for the recruitment of MLL1 associated complex to the context of ARE.

BAP18 enhances AR/AR-V7-induced transactivation in prostate cancer

As AR is expressed in the greater number of both androgen-dependent prostate cancer (ADPC) and CRPC, and a amount of AR binding sites have been identified in ADPC and CRPC (38,39), thus the AR-mediated pathways play important roles in both ADPC and CRPC. On the other hand, under conditions of androgen depletion, the synthesis of AR splicing variants (AR-Vs) carrying C-terminal truncation provides a compelling mechanism for the progression of CRPC to androgen deprivation therapy (ADT). At least 20 AR-Vs has been identified in CRPC cell lines or PCa samples. AR-V7 is a putative AR splicing variant and is often selected as a candidate for research on CRPC (5,6). Our results suggest that BAP18 is involved in enhancing AR-mediated transactivation in the presence of ligand (5α-dihydrotestosterone, DHT). Importantly, BAP18 specifically increases transcriptional activity induced by ARAF-1 as well as AR-V7 in a ligand-independent manner (Figure 3A–E). RNA-seq analysis data demonstrate that BAP18 participates in modulating globle AR-induced gene expression in the absence or presence of DHT, indicating that BAP18 may be involved in regulation of genome-wide AR-mediated transcription (Figure 3H–K). Knockdown of BAP18 attenuates the expression of a subset of AR target genes, such as *KLK4*, *FKBP5*, *FASN* (36), *UBE2C*, which are crucial for the progression of ADPC and CRPC (Figure 4A–B). Interestingly, it has been defined that AR selectively and directly enhances M-phase cell-cycle genes, including *UBE2C* in androgen-independent cells to promote CRPC growth (4,35,40). Our results together with those from Wang *et al*. show that BAP18 may act as a co-activator of AR/AR-V7 to contribute to ADPC and CRPC progression through the modulation of a subset of AR target genes.

We observed a robust effect of BAP18 depletion on cell growth and proliferation in presence or absence of DHT. In addition, the significant differences in BAP18 expression detected between BPH and prostate cancer samples strongly proposed that BAP18 highly expressed in prostate cancer may play a role in tumor initiation and progression. The previous studies showed that increased histone H4K16ac and H3K4me3 are epigenetic signature of cellular proliferation (41,42). In addition, overexpression of MOF is correlated with tumor growth, oncogenic transformation, and prostate cancer progression (41,43). It has been previously demonstrated that MLL1 complex, including WDR5, Ash2L or Menin plays a crucial role in prostate cancer initiation or CRPC progression (19,20). Our data suggest that BAP18 facilitates the recruitment of MLL1 complex, including MLL1, MOF, Ash2L and Menin to the context of AR target genes, resulting in high levels of H3K4me3 and H4K16ac to promote a subset of AR/AR-Vs target gene transcription. Thus, activation of this signaling cascade promotes the increased or abnormal cell growth and proliferation of prostate cancer or development of CRPC (Figure 7G). Further studies will examine whether BAP18 is involved in modulation of transcriptional activity induced by other steroid hormone receptors and participates in other hormone-related human tumors.

Collectively, our observations identify BAP18 as a crucial co-activator of AR/AR-V7 function and have uncovered a mechanism in which BAP18 facilitates the recruitment of MLL1 subcomplex to the context of AR target genes, resulting in histone modification alteration to regulate AR-dependent gene activation. Our findings have demonstrated that BAP18 plays a key role in prostate cancer cell proliferation and CRPC progression, and we wonder whether BAP18 expression would be utilized as a novel biomarker for prostate cancer prognosis and whether BAP18 could be a potential therapeutic target for patients with prostate cancer and CRPC.

ACCESSION NUMBERS

RNA-seq data in this study have been deposited in the NCBI Sequence Read Archive (SRA) database under accession number SRP074464.

SUPPLEMENTARY DATA

Supplementary Data are available at NAR Online.

ACKNOWLEDGEMENTS

The authors appreciate Dr Yunlong Huo and Tao Wen for helpful technique support. The authors thank Dr Shigeaki Kato (Soma Central Hospital, Fukusima, Japan) for the AR expression plasmid and pARE-tk-luc reporter. The authors also thank BGI-Shenzhen, Shenzhen, China for RNA-seq analysis and Beijing Ori-Gene Technology Co., LTD Company for technology support.

FUNDING

973 Program Grant from the Ministry of Science and Technology of China [2013CB945201]; National Natural Science Foundation of China [30871390, 31171259, 31271364 for Y.Z., 31401115 for C.W., 81502438 for T.Z., 31300963 for X.S.]; Ministry of Education fund innovation team [IRT 13101]; Ministry of Education Science and technology research [No 213008A]. Funding for open access charge: 973 Program Grant from the Ministry of Science and Technology of China [2013CB945201]; National Natural Science

Foundation of China [30871390, 31171259, 31271364 for Y.Z., 31401115 for C.W., 81502438 for T.Z., 31300963 for X.S.]; Ministry of Education fund innovation team [IRT 13101]; Ministry of Education Science and technology research [No 213008A].
Conflict of interest statement. None declared.

REFERENCES

1. Welsbie,D.S., Xu,J., Chen,Y., Borsu,L., Scher,H.I., Rosen,N. and Sawyers,C.L. (2009) Histone deacetylases are required for androgen receptor function in hormone-sensitive and castrate-resistant prostate cancer. *Cancer Res.*, **69**, 958–966.
2. Cai,C., He,H.H., Chen,S., Coleman,I., Wang,H., Fang,Z., Chen,S., Nelson,P.S., Liu,X.S., Brown,M. *et al.* (2011) Androgen receptor gene expression in prostate cancer is directly suppressed by the androgen receptor through recruitment of lysine-specific demethylase 1. *Cancer Cell*, **20**, 457–471.
3. Nwachukwu,J.C., Mita,P., Ruoff,R., Ha,S., Wang,Q., Huang,S.J., Taneja,S.S., Brown,M., Gerald,W.L., Garabedian,M.J. *et al.* (2009) Genome-wide impact of androgen receptor trapped clone-27 loss on androgen-regulated transcription in prostate cancer cells. *Cancer Res.*, **69**, 3140–3147.
4. Wang,Q., Li,W., Zhang,Y., Yuan,X., Xu,K., Yu,J., Chen,Z., Beroukhim,R., Wang,H., Lupien,M. *et al.* (2009) Androgen receptor regulates a distinct transcription program in androgen-independent prostate cancer. *Cell*, **138**, 245–256.
5. Li,Y., Chan,S.C., Brand,L.J., Hwang,T.H., Silverstein,K.A. and Dehm,S.M. (2013) Androgen receptor splice variants mediate enzalutamide resistance in castration-resistant prostate cancer cell lines. *Cancer Res.*, **73**, 483–489.
6. Lu,J., der Steen,T.V. and Tindall,D.J. (2015) Are androgen receptor variants a substitute for the full-length receptor? *Nat. Rev. Urol.*, **12**, 137–144.
7. Xu,K., Shimelis,H., Linn,D.E., Jiang,R., Yang,X., Sun,F., Guo,Z., Chen,H., Li,W., Chen,H. *et al.* (2009) Regulation of androgen receptor transcriptional activity and specificity by RNF6-induced ubiquitination. *Cancer Cell*, **15**, 270–282.
8. Perissi,V., Aggarwal,A., Glass,C.K., Rose,D.W. and Rosenfeld,M.G. (2004) A corepressor/coactivator exchange complex required for transcriptional activation by nuclear receptors and other regulated transcription factors. *Cell*, **116**, 511–526.
9. Lessard,J.A. and Crabtree,G.R. (2010) Chromatin regulatory mechanisms in pluripotency. *Annu. Rev. Cell Dev. Biol.*, **26**, 503–532.
10. Taverna,S.D., Li,H., Ruthenburg,A.J., Allis,C.D. and Patel,D.J. (2007) How chromatin-binding modules interpret histone modifications: lessons from professional pocket pickers. *Nat. Struct. Mol. Biol.*, **14**, 1025–1040.
11. Heemers,H.V. and Tindall,D.J. (2007) Androgen receptor (AR) coregulators: a diversity of functions converging on and regulating the AR transcriptional complex. *Endocr. Rev.*, **28**, 778–808.
12. Qi,J., Tripathi,M., Mishra,R., Sahgal,N., Fazli,L., Ettinger,S., Placzek,W.J., Claps,G., Chung,L.W., Bowtell,D. *et al.* (2013) The E3 ubiquitin ligase Siah2 contributes to castration-resistant prostate cancer by regulation of androgen receptor transcriptional activity. *Cancer Cell*, **23**, 332–346.
13. Zippo,A., Serafini,R., Rocchigiani,M., Pennacchini,S., Krepelova,A. and Oliviero,S. (2009) Histone crosstalk between H3S10ph and H4K16ac generates a histone code that mediates transcription elongation. *Cell*, **138**, 1122–1136.
14. Qi,W., Wu,H., Yang,L., Boyd,D.D. and Wang,Z. (2007) A novel function of caspase-8 in the regulation of androgen-receptor-driven gene expression. *EMBO J.*, **26**, 65–75.
15. Mahajan,N.P., Liu,Y., Majumder,S., Warren,M.R., Parker,C.E., Mohler,J.L., Earp,H.S. and Whang,Y.E. (2007) Activated Cdc42-associated kinase Ack1 promotes prostate cancer progression via androgen receptor tyrosine phosphorylation. *Proc. Natl. Acad. Sci. U.S.A.*, **104**, 8438–8443.
16. Lee,J.H., Isayeva,T., Larson,M.R., Sawant,A., Cha,H.R., Chanda,D., Chesnokov,I.N. and Ponnazhagan,S. (2015) Endostatin: A novel inhibitor of androgen receptor function in prostate cancer. *Proc. Natl. Acad. Sci. U.S.A.*, **112**, 1392–1397.
17. Yokoyama,A., Somervaille,T.C., Smith,K.S., Rozenblatt-Rosen,O., Meyerson,M. and Cleary,M.L. (2005) The menin tumor suppressor protein is an essential oncogenic cofactor for MLL-associated leukemogenesis. *Cell*, **123**, 207–218.
18. Dou,Y., Milne,T.A., Tackett,A.J., Smith,E.R., Fukuda,A., Wysocka,J., Allis,C.D., Chait,B.T., Hess,J.L. and Roeder,R.G. (2005) Physical association and coordinate function of the H3 K4 methyltransferase MLL1 and the H4 K16 acetyltransferase MOF. *Cell*, **121**, 873–885.
19. Kim,J.Y., Banerjee,T., Vinckevicius,A., Luo,Q., Parker,J.B., Baker,M.R., Radhakrishnan,I., Wei,J.J., Barish,G.D. and Chakravarti,D. (2014) A role for WDR5 in integrating threonine 11 Phosphorylation to Lysine 4 Methylation on Histone H3 during androgen signaling and in prostate cancer. *Mol. Cell*, **54**, 613–625.
20. Malik,R., Khan,A.P., Asangani,I.A., Cieslik,M., Prensner,J.R., Wang,X., Iyer,M.K., Jiang,X., Borkin,D., Escara-Wilke,J. *et al.* (2015) Targeting the MLL complex in castration-resistant prostate cancer. *Nat. Med.*, **21**, 344–352.
21. Vermeulen,M., Eberl,H.C., Matarese,F., Marks,H., Denissov,S., Butter,F., Lee,K.K., Olsen,J.V., Hyman,A.A., Stunnenberg,H.G. *et al.* (2010) Quantitative interaction proteomics and genome-wide profiling of epigenetic histone marks and their readers. *Cell*, **142**, 967–980.
22. Boyer,L.A., Latek,R.R. and Peterson,C.L. (2004) The SANT domain: a unique histone-tail-binding module? *Nat. Rev. Mol. Cell Biol.*, **5**, 158–163.
23. Yadon,A.N. and Tsukiyama,T. (2011) SnapShot: Chromatin remodeling: ISWI. *Cell*, **144**, 453–453.
24. Zhao,Y., Lang,G., Ito,S., Bonnet,J., Metzger,E., Sawatsubashi,S., Suzuki,E., Le Guezennec,X., Stunnenberg,H.G., Krasnov,A. *et al.* (2008) A TFTC/STAGA module mediates histone H2A and H2B deubiquitination, coactivates nuclear receptors, and counteracts heterochromatin silencing. *Mol. Cell*, **29**, 92–101.
25. Zhao,Y., Takeyama,K., Sawatsubashi,S., Ito,S., Suzuki,E., Yamagata,K., Tanabe,M., Kimura,S., Fujiyama,S., Ueda,T. *et al.* (2009) Corepressive action of CBP on androgen receptor transactivation in pericentric heterochromatin in a Drosophila experimental model system. *Mol. Cell. Biol.*, **29**, 1017–1034.
26. Takeyama,K., Ito,S., Yamamoto,A., Tanimoto,H., Furutani,T., Kanuka,H., Miura,M., Tabata,T. and Kato,S. (2002) Androgen-dependent neurodegeneration by polyglutamine-expanded human androgen receptor in Drosophila. *Neuron*, **35**, 855–864.
27. Zhao,Y., Goto,K., Saitoh,M., Yanase,T., Nomura,M., Okabe,T., Takayanagi,R. and Nawata,H. (2002) Activation function-1 domain of androgen receptor contributes to the interaction between subnuclear splicing factor compartment and nuclear receptor compartment. Identification of the p102 U5 small nuclear ribonucleoprotein particle-binding protein as a coactivator for the receptor. *J. Biol. Chem.*, **277**, 30031–30039.
28. Wang,C., Sun,H., Zou,R., Zhou,T., Wang,S., Sun,S., Tong,C., Luo,H., Li,Y., Li,Z. *et al.* (2015) MDC1 functionally identified as an androgen receptor co-activator participates in suppression of prostate cancer. *Nucleic Acids Res.*, **43**, 4893–4908.
29. Cai,Y., Jin,J., Swanson,S.K., Cole,M.D., Choi,S.H., Florens,L., Washburn,M.P., Conaway,J.W. and Conaway,R.C. (2010) Subunit composition and substrate specificity of a MOF-containing histone acetyltransferase distinct from the male-specific lethal (MSL) complex. *J. Biol. Chem.*, **285**, 4268–4272.
30. Remacle,A.G., Golubkov,V.S., Shiryaev,S.A., Dahl,R., Stebbins,J.L., Chernov,A.V., Cheltsov,A.V., Pellecchia,M. and Strongin,A.Y. (2012) Novel MT1-MMP small-molecule inhibitors based on insights into hemopexin domain function in tumor growth. *Cancer Res.*, **72**, 2339–2349.
31. Zou,R., Zhong,X., Wang,C., Sun,H., Wang,S., Lin,L., Sun,S., Tong,C., Luo,H., Gao,P. *et al.* (2015) MDC1 Enhances Estrogen Receptor-mediated Transactivation and Contributes to Breast Cancer Suppression. *Int. J. Biol. Sci.*, **11**, 992–1005.
32. Matsumoto,T., Sakari,M., Okada,M., Yokoyama,A., Takahashi,S., Kouzmenko,A. and Kato,S. (2013) The androgen receptor in health and disease. *Annu. Rev. Physiol.*, **75**, 201–224.
33. Grasso,C.S., Wu,Y.M., Robinson,D.R., Cao,X., Dhanasekaran,S.M., Khan,A.P., Quist,M.J., Jing,X., Lonigro,R.J., Brenner,J.C. *et al.* (2012) The mutational landscape of lethal castration-resistant prostate cancer. *Nature*, **487**, 239–243.

34. Sahu,B., Laakso,M., Ovaska,K., Mirtti,T., Lundin,J., Rannikko,A., Sankila,A., Turunen,J.P., Lundin,M., Konsti,J. *et al.* (2011) Dual role of FoxA1 in androgen receptor binding to chromatin, androgen signalling and prostate cancer. *EMBO J.*, **30**, 3962–3976.
35. Wang,H., Zhang,C., Rorick,A., Wu,D., Chiu,M., Thomas-Ahner,J., Chen,Z., Chen,H., Clinton,S.K., Chan,K.K. *et al.* (2011) CCI-779 inhibits cell-cycle G2-M progression and invasion of castration-resistant prostate cancer via attenuation of UBE2C transcription and mRNA stability. *Cancer Res.*, **71**, 4866–4876.
36. Migita,T., Ruiz,S., Fornari,A., Fiorentino,M., Priolo,C., Zadra,G., Inazuka,F., Grisanzio,C., Palescandolo,E., Shin,E. *et al.* (2009) Fatty acid synthase: a metabolic enzyme and candidate oncogene in prostate cancer. *J. Natl. Cancer Inst.*, **101**, 519–532.
37. Tremblay,V., Zhang,P., Chaturvedi,C.P., Thornton,J., Brunzelle,J.S., Skiniotis,G., Shilatifard,A., Brand,M. and Couture,J.F. (2014) Molecular Basis for DPY-30 Association to COMPASS-like and NURF Complexes. *Structure*, **22**, 1821–1830.
38. Sharma,N.L., Massie,C.E., Ramos-Montoya,A., Zecchini,V., Scott,H.E., Lamb,A.D., MacArthur,S., Stark,R., Warren,A.Y., Mills,I.G. *et al.* (2013) The androgen receptor induces a distinct transcriptional program in castration-resistant prostate cancer in man. *Cancer Cell*, **23**, 35–47.
39. Hu,R., Lu,C., Mostaghel,E.A., Yegnasubramanian,S., Gurel,M., Tannahill,C., Edwards,J., Isaacs,W.B., Nelson,P.S., Bluemn,E. *et al.* (2012) Distinct transcriptional programs mediated by the ligand-dependent full-length androgen receptor and its splice variants in castration-resistant prostate cancer. *Cancer Res.*, **72**, 3457–3462.
40. Chen,Z., Zhang,C., Wu,D., Chen,H., Rorick,A., Zhang,X. and Wang,Q. (2011) Phospho-MED1-enhanced UBE2C locus looping drives castration-resistant prostate cancer growth. *EMBO J.*, **30**, 2405–2419.
41. Gupta,A., Guerin-Peyrou,T.G., Sharma,G.G., Park,C., Agarwal,M., Ganju,R.K., Pandita,S., Choi,K., Sukumar,S., Pandita,R.K. *et al.* (2008) The mammalian ortholog of Drosophila MOF that acetylates histone H4 lysine 16 is essential for embryogenesis and oncogenesis. *Mol. Cell. Biol.*, **28**, 397–409.
42. Metzger,E., Imhof,A., Patel,D., Kahl,P., Hoffmeyer,K., Friedrichs,N., Muller,J.M., Greschik,H., Kirfel,J., Ji,S. *et al.* (2010) Phosphorylation of histone H3T6 by PKCbeta(I) controls demethylation at histone H3K4. *Nature*, **464**, 792–796.
43. Jaganathan,A., Chaurasia,P., Xiao,G.Q., Philizaire,M., Lv,X., Yao,S., Burnstein,K.L., Liu,D.P., Levine,A.C. and Mujtaba,S. (2014) Coactivator MYST1 regulates nuclear factor-kappaB and androgen receptor functions during proliferation of prostate cancer cells. *Mol. Endocrinol.*, **28**, 872–885.